Egypt. J. Chem. **Vol. 68**, No. 1 pp. 507- 518 (2025)

Egyptian Journal of Chemistry

http://ejchem.journals.ekb.eg/

Anti-Cancer And Safety Profiles Of Doxorubicin-Loaded Kaolinite Against Ehrlich Solid Tumor

Fatma Al-Zahraa Sayed[a,c*], Ayman S. Mohamed[b], Heba Mohamed Fahmy[c]

[a] *School of Biotechnology, Badr University in Cairo, Badr City, Cairo 11829, Egypt.*

[b] *Zoology Department, Faculty of Science, Cairo University, Giza, Egypt.*

[c] *Biophysics Department, Faculty of Science, Cairo University, Giza, Egypt.*

Abstract

The current conventional cancer therapies do not offer a radical cure and frequently result in significant adverse effects. The present study presents an alternative by repackaging doxorubicin, a commonly used chemotherapy drug, into doxorubicin-loaded kaolinite as a treatment for breast cancer. We characterized the synthesized nanoparticles using a transmission electron microscope (TEM), dynamic light scattering (DLS), and zeta potential. After 18 days of treatment, we assessed the anti-cancer efficacy based on tumor weight and tumor tissue histopathology. Furthermore, the cyto/genotoxic effects of the treatment on the liver were evaluated via oxidative stress measurement, histopathological examination, and a comet assay. Additionally, we assessed the hemocompatibility of the nanoparticles by measuring the hemolysis percentage. The characterization techniques confirmed that the nanoparticles demonstrated acceptable physico-chemical characteristics. Moreover, the histopathological examination of the tumor tissue corresponds with the reduction in tumor size. Furthermore, the formulation reduced cancer-related stress on the liver by reducing oxidative stress and subsequent inflammation, preventing metastasis of tumor cells, and reducing DNA damage. Moreover, the hemolysis test revealed its blood biocompatibility. These results strengthen the formulation's anti-cancer efficacy and safety, providing more biocompatible and benign cancer treatment alternatives. The formula's clinical effectiveness must be confirmed by further clinical studies.

Keywords: Kaolinite,Kaolin,Cancer,Ehrlich tumor,Doxorubicin,Hemolysis

1. Introduction

Cancer, a complicated disease, has long presented problematic therapeutic challenges [1]. Chemotherapy using doxorubicin is commonly used as the first-line treatment for breast cancer, one of the most prevalent cancer types [2]. However, chemotherapy is limited to specific grades of the disease, may induce resistance by the tumor cells, and may cause unpleasant side effects that may be life-threatening in some cases [3]. Numerous studies have proven nanoparticles' (NPs') powerful therapeutic efficacy and ability to prevent undesirable side effects, resulting in their impending usage in clinical settings [4]. Medical and pharmaceutical societies favor nanoparticles in cancer therapy for several reasons [5]. NPs can exploit the distorted structure of tumor cells. For example, they use enhanced permeability and retention effects (EPR) to accumulate specifically in malignant cells, targeting them passively [6]. EPR allows drugs to accumulate in tumors, extend their blood circulation, boost antitumor immunity, and enable sustained release of drugs [7, 8]. Additionally, NPs can be functionalized with ligands that selectively bind to target cells, which helps transport cargo and accomplish active targeting [1]. Moreover, nanoparticles can encapsulate and transport drugs that cannot pass through the cell membrane. [9, 10]. Nanoparticles can take advantage of the fact that cancer cells get their energy from glycolysis, which induces an acidic environment within the cells, enabling the release of drugs according to pH stimulation [11]. However, the challenge remains to identify the optimal carrier among various effective anticancer nanoparticles. This optimal carrier must meet criteria such as safety, biocompatibility, circulation lifetime, cost, solubility, release profiles, and encapsulation efficiency [6]. Clay minerals, as a promising treatment for cancer, have many advantages for being either a drug carrier or inherently killing cancer cells [12]. Kaolinite, also known as kaolin, has the chemical formula Al2Si2O5(OH)4 and is a widely available and cost-effective nano clay with a natural multiple nanolayer structure. Additionally, kaolinite possesses a large surface area containing abundant active hydroxyl groups and a high adsorption capacity, enabling interaction with various species and functional groups. This property makes them highly efficient at loading a variety of substances. Also, kaolinite possesses anti-oxidants and antibacterial and anti-inflammatory properties [13–17]. Moreover, kaolinite can provide a pH-dependent drug release, allowing the concentration of drug within the acidic tumors and reducing off-target systemic toxicity [16]. Kaolinite also has the special advantage of being used as an excipient or active pharmaceutical component, ascertaining its compatibility [13]. Kaolinite or kaolinite-based composites have been used for cancer therapy either as a delivery system for many medications, such as doxorubicin, 5-fluorouracil, and oxaliplatin, or due to their synergistic properties [16]. For instance, a study by Zhang and his coworkers [14] explored the anticancer effects of doxorubicin-loaded kaolinite, which was first intercalated with various substances, including dimethyl sulfoxide (DMSO) and methanol, to increase the basal spacing of kaolinite and achieve a high loading efficiency. Intercalation is crucial for expanding the interlayer spaces between the different kaolinite layers, providing more drug-loading

*Corresponding author e-mail: fatma.elzhraa@buc.edu.eg.; (Fatma Al-Zahraa Sayed).

Receive Date: 30 April 2024,Revise Date: 21 May 2024, Accept Date: 27 May 2024

DOI: 10.21608/ejchem.2024.286346.9665

sites [14]. The MTS (3-(4,5-dimethylthiazol-2-yl)-5-(3-carboxymethoxyphenyl)-2-(4-sulfophenyl)-2H-tetrazolium) assay revealed that applying the previous materials to different human cancer cell lines reduced their viability in a dose-dependent manner. In vivo, experiments with kaolinite have demonstrated successful targeted drug delivery and cancer cell combat, such as the study done by Zhang and his colleagues [18], who investigated the anticancer effect of the actively targeted composite KI@Dox-Mn3O4@kaolin C12N for treating thyroid cancer in nude mice. The delivery of 5-fluorouracil loaded in kaolinite nanotubes was investigated by Abukhadra and Fadl Allah, [19] who found that the carrier achieved a sustained release and showed biocompatibility against the normal cell line mouse fibroblast (L929). Moreover, kaolinite showed intrinsic anticancer efficacy, as demonstrated by [20, 21], showed that the composites, Au@kaolin and kaolin@chitosan@gold, killed cancer cell lines depending on the dose, as revealed by MTT (3-(4,5-dimethylthiazol-2-yl)-2,5-diphenyltetrazolium bromide) tetrazolium reduction assay. In a recent study by Zhang [22], the nanocomposite Au@kaolinite exhibited anticancer effects against ovarian cancer in vitro and demonstrated antiproliferative and anti-inflammatory properties against uterine adenomyosis. Studying the therapeutic effect of a treatment is crucial, but studying its side effects is equally important. Detecting cyto/genotoxic effects is crucial for validating the use of the treatment. One standard method is measuring oxidative stress markers, which provides insights into the subsequent inflammation and DNA damage in tissues [23]. A standard method of determining DNA damage is the comet assay, a commonly used technique for studying the genotoxicity of compounds, including synthesized nanoparticles [24]. Moreover, the hemolysis test as a measurement of RBCs damage was performed, which is essential because the destruction of red blood cells is an important toxicity indicator [25,26]. Kaolinite-related in vivo anticancer studies are scarce, with limited types of animal models and a lack of such details. Additionally, the potential of doxorubicin-loaded kaolinite against breast cancer models has not been thoroughly evaluated, although it is one of the leading death types. Hence, the current study aims to address this gap by investigating the anticancer effects of doxorubicin-loaded kaolinite against Ehrlich solid tumors, a common breast cancer model in mice. This topic has yet to be extensively explored. The formulation was prepared by intercalating raw kaolinite with DMSO, followed by methanol, and then loaded with doxorubicin via electrostatic interaction. The formulation was characterized using a range of tests, including TEM, DLS, and zeta potential. The mice were inoculated subcutaneously with the Ehrlich solid tumor, and the size was monitored for 18 days. We further assessed the formulation's effect using a comprehensive histopathological examination of the tumor. Furthermore, the safety profiles were assessed using oxidative stress, histological examination, and comet assay. We also assessed hemocompatibility using a hemolysis assay, ensuring a thorough evaluation of the formulation's safety.

2. Materials and Method

2.1. Materials

Kaolinite-methanol(CH3OH)-dimethylsulphoxide(DMSO), purchased from Sigma Aldrich, USA- doxorubicin, purchased from Al-Hikma pharmaceutical company, Egypt- Superoxide dismutase(SOD), Glutathione reduced(GSH), and Malondialdehyde(MDA), purchased from Biodiagnostics company, Egypt.

2.2. Methods

2.2.1. Preparation of doxorubicin-loaded kaolinite

The preparation of kaolinite-loaded doxorubicin nanoparticles included three steps, according to Zhang [14]. The raw kaolinite was intercalated with DMSO by dispersing 15 g of kaolinite into 60 ml at 60 ^{o}C for 12 hours. Then, the mixture was centrifuged, and 5 g of pellets were dispersed in 100 ml of methanol, which was displaced daily for seven days. Moreover, the mixture was centrifuged, and the pellets were evaporated at room temperature, forming a powder of methanol-intercalated kaolinite. 5 mg of the methanol-intercalated kaolinite was dispersed in 6 ml of doxorubicin (0.5 mg/ml) and left under stirring for 24 hours. Then, the solution was centrifuged to remove excess doxorubicin, and the loading efficiency was determined using a UV-Vis spectrophotometer at a wavelength of 485nm, according to the following equation developed by Monem [27]:

$$\text{Loading efficiency (\%)} = \frac{Total\ drug\ concentration - concentration\ of drug\ in\ supernatant}{Total\ drug\ concentration} x\ 100 \quad (1)$$

2.2.2. Characterization of nanoparticles:

The nanoparticles were characterized using a TEM (HR-TEM; JEM-2100, JEOL, Tokyo, Japan) to determine their size and shape. The Zeta Potential/Particle Sizer NICOMPTM380ZLS (USA) DLS device determined the hydrodynamic diameter and surface charge.

2.2.3. In vitro drug release

The drug release experiment was performed at two distinct pH levels (5.5 and 7.4). Briefly, 2 mg of the formulation was dispersed into 3 ml in a dialysis bag and placed into 15 ml of each buffer solution. Over 30 hours, the release rate was examined at regular intervals using a UV-Vis spectrophotometer at a wavelength of 485nm. Cumulative drug release was calculated by the following equation developed by Li [28]:

$$Cumulative\ release = \frac{\text{drug conc. outside the dialysis bag x 15 ml}}{\text{drug conc. inside dialysis bag x 3 ml}}\ x\ 100 \quad (2)$$

2.2.4. The in vivo study and the treatment protocol

The in vivo experiment involved 40 female CD1 mice obtained from a local supplier. At two months, the mice had an average weight of 20–25 g. The Institutional Animal Care and Use Committee (CU-IACUC) established animal management and utilization protocols. The mice were grouped into ten each, subjected to a 12-hour dark/light cycle, and maintained in a temperature-controlled environment. They had unimpeded access to nutrition and water. Before the experiment began, the animals could acclimate for one week.

2.2.5. Acute toxicity testing (LD50) and animal grouping

An acute toxicity study provides specific data on a pharmacological substance's lethal dose (LD_{50}), therapeutic index, and safety level. The lethal dose (LD_{50}), which is the dosage that results in the death of 50% of the population of test animals, was determined [29]. After a fasting period, the mice were divided into four groups, each containing two mice for treatment. The mice were given dosages of doxorubicin-loaded kaolinite at 10, 100, 300, and 600 mg/kg, respectively. After the injection, the mice were evaluated for two hours and monitored for 24 hours. During this phase, various behaviors and signs were observed, including paw licking, weariness, partially solid feces, excessive salivation, writhing, and decreased hunger [30]. The LD_{50} was determined using the following equation:

$$LD_{50}=(M0+M1)/2 \quad (3)$$

M0 is the highest dose that causes no mortality.

M1 is the highest dose that causes mortality.

Afterward, the experimental groups were divided into four groups as indicated in table.1.

Table 1 displays the animal groups included in the study, along with the distinct treatments they received.

Animal groups	Treatment
G1	Naïve mice received 200µl of saline intraperitoneally twice a week.
G2	They were injected intraperitoneally with 200 µl of saline twice a week.
G3	Injected intraperitoneally with doxorubicin (200µl, 2 mg/kg) once a week [31].
G4	They were injected intraperitoneally with 200 µl of doxorubicin-loaded kaolinite nanoparticles (450 mg/kg).

2.2.6. Inoculation of mice with the Ehrlich solid carcinoma

To form solid tumors, mice in the G2, G3, and G4 groups received a subcutaneous injection of two million tumor cells (0.2 ml) into their right flank. The mice developed a solid tumor measuring 0.3-0.6 cm^3 within ten days, and the experiment was extended for another 18 days of treatment [32]. After the experiment, the mice were euthanized via exsanguination, and the tumors and livers were excised for further use.

2.2.7. Histopathological examination

The tumor and liver tissues were preserved in 10% formalin, embedded in paraffin blocks, and sliced into 5µm-thick slices. The specimens were stained with Hematoxylin and eosin (H&E). The stained sections were photographed using a digital camera (Leica DMC 4500, Germany) connected to a light microscope (Leica DM4B, Germany).

2.2.8. Oxidative stress measurements

Lipid peroxidation measurement was developed according to Ohkawa [33]. The method involves reacting malondialdehyde (MDA) with thiobarbituric acid (TBA) at 95 °C for 30 minutes under acidic conditions. The resulting pink material can be detected at 534 nm, with the intensity of the color corresponding to the concentration of MDA.

To assay glutathione reduced (GSH), the manufacturer's instructions and a method developed by Beutler [34] were followed. This method involves measuring the absorbance at 405 nm of a yellow product formed by the reaction of glutathione with 5,5 dithiobis (2-nitrobenzoic acid) (DTNB). The intensity of the yellow product corresponds to higher levels of GSH.

Furthermore, the SOD assay provided by Nishikimi [35] relies on the enzyme's ability to prevent the reduction of nitroblue tetrazolium (NBT) dye mediated by phenazine methosulfate (PMS). According to the purchased SOD assay kit, the change in absorbance within 5 minutes was measured at 560 nm, and then the percent of inhibition was calculated.

2.2.9. Comet assay

The comet assay (single-cell gel electrophoresis) was used to analyze and quantify DNA damage in liver tissue. The tissue was homogenized, and the cell suspension was centrifuged at (700 x g) for 10 minutes at a temperature of 4 ^oC. The re-suspension of the cells was then followed in a cold buffer, embedded in an agarose gel, and lysed to release DNA, stained with a dye to be visualized. The visualization of slides was achieved by the use of a fluorescence microscope of 400x magnification linked to a CCD camera. The degree of DNA damage was evaluated using metrics such as the percentage of damage, comet tail length, DNA damage percentage, tail moments, and olive tail moments. The analysis system was the Comet Image Analysis System (Kinetic Imaging Ltd., Liverpool, UK).

2.2.10. Blood biocompatibility assay

The erythrocyte toxicity assay was carried out according to Mazzarino [25]. Briefly, 950 µl of saline containing varying concentrations of doxorubicin-loaded kaolinite nanoparticles (6.25, 12.5, 25, 50, and 100 µg/ml) was mixed with 50 µl of the erythrocyte stock. The mixture was then incubated for one hour at 37^oC. Centrifugation was used to extract intact red blood cells (RBCs) for five minutes at 10,000 rpm. After that, a measurement of the supernatant's absorbance at 540 nm was made. Distilled water was used as a positive control (100% lysis), and saline solution (0.9% NaCl) was used as a negative control (0% lysis). The following equation was used to compute the hemolysis rate.

$$Hemolysis\ rate\ (\%) = \frac{D_t - D_{nc}}{D_{pc} - D_{nc}}\ x\ 100 \quad (4)$$

The absorbance of the tested sample, negative control, and positive control are represented by Dt, Dnc, and Dpc, respectively [36]. The experiments were conducted three times.

2.2.11. Statistical analysis

Statistical analysis was conducted using a one-way ANOVA test. The data were presented as the average value plus or minus the standard deviation. The statistical analysis was conducted using SPSS version 26. The various significance levels were denoted as (P *** ≤0.001, P** ≤0.01, and P* ≤ 0.05) in comparison to the positive control group.

3. Results

3.1. Preparation and characterization of doxorubicin-loaded kaolinite

The doxorubicin-loaded kaolinite nanoparticles were prepared by intercalating raw kaolinite with DMSO, followed by methanol, and then loaded with doxorubicin, achieving a loading efficiency of 73%. The nanoparticles were then meticulously characterized with TEM, which revealed a platy hexagonal morphology and an average size of 55 ± 8.85 nm. The TEM image also indicates that the nanoparticles exhibited low crystallinity, as depicted in Fig. 1. Moreover, the DLS (Fig. 2) shows that the bare nano kaolinite had a hydrodynamic diameter of 95nm. After doxorubicin loading, the diameter increased to 151nm. Furthermore, the zeta potential (Fig. 3) varied from -37 mV in bare nano kaolinite to 10 mV in doxorubicin-loaded kaolinite

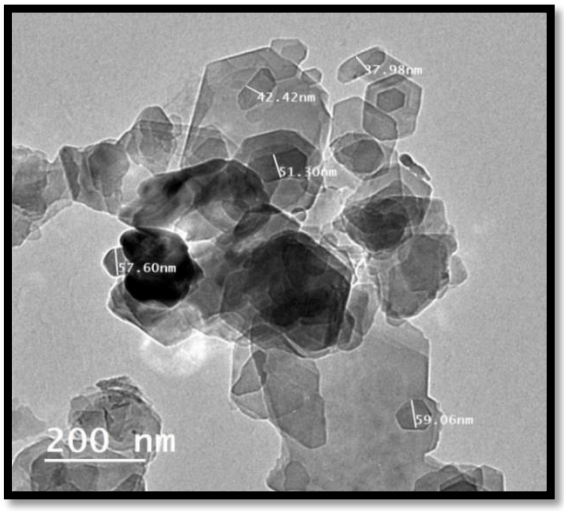

Fig. 1. TEM of methanol intercalated kaolinite

.

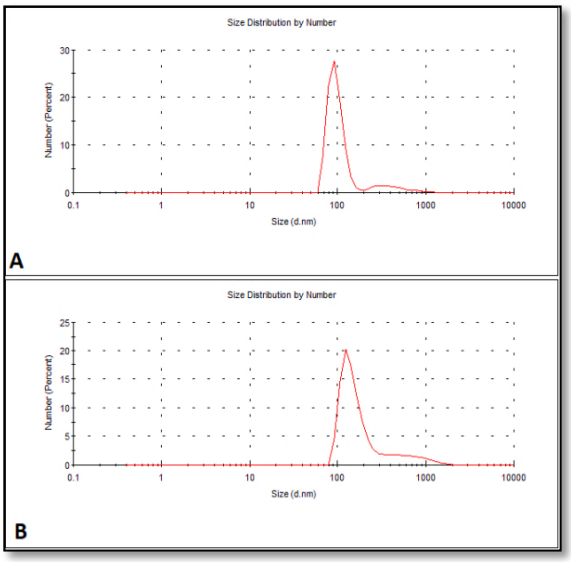

Fig.2. Dynamic light scattering data for A: bare nano kaolinite and B: doxorubicin-loaded kaolinite.

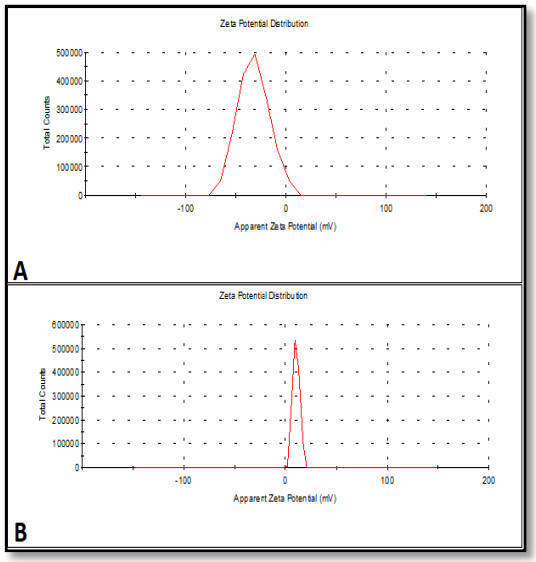

Fig.3. Zeta potential data for A: bare nano kaolinite and B: doxorubicin-loaded kaolinite.

3.2. In *vitro* drug release:

The drug release investigation was performed at pH 7.4 and 5.5 to replicate the pH values of both blood and tumors, respectively. Based on Figure 4, the drug release rate was markedly greater at pH 5.5, reaching 33%, in contrast to 10% at pH 7.4.

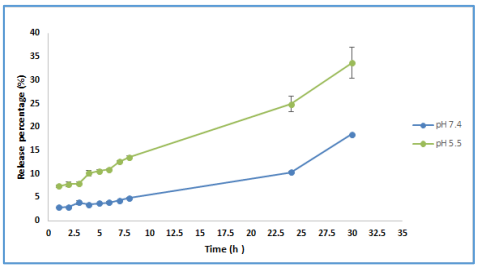

Fig.4. In *vitro* drug release at pH of 5.5 and 7.4.

3.3. Anti-tumor efficacy of doxorubicin-loaded kaolinite

3.3.1. Effect on tumor mass:

The Ehrlich solid tumor was used to mimic human breast cancer—the in vivo experiment compared the effect of doxorubicin-loaded kaolinite to doxorubicin alone. Figure 4 shows a significant decrease in tumor mass in the G3 and G4 groups compared to the G2 group. Notably, the reduction in the G4 group, which received doxorubicin-loaded kaolinite treatment, was 41.49% more significant (P *** ≤ 0.001) than in the G3 group, which received free doxorubicin.

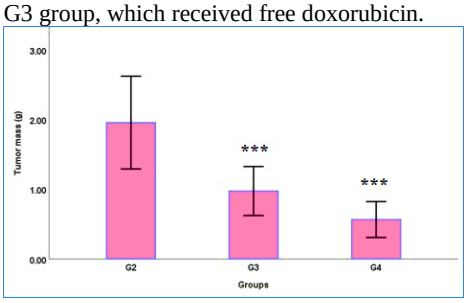

Fig.5. Tumor mass of G2: Saline, G3: doxorubicin, and G4: doxorubicin-loaded kaolinite.

3.3.2. Effect on tumor tissues:

Histological alterations in the Ehrlich tumor tissues, as shown in Figure 6, corroborated the findings above. The Ehrlich tumor group (G2) displayed viable, undifferentiated tumor cells with marked pleomorphism, hyperchromatism, an increased nuclear-cytoplasmic ratio, prominent nucleoli, and frequent mitosis. The photomicrograph of (G3), which was administered with doxorubicin, shows remaining viable tumor cells with notable features of malignancy in the lower right corner (*), with fibroblasts and fibrosis encroaching on tumor cells (arrows). In contrast, the group of mice (G4) that received treatment with doxorubicin-loaded kaolinite replaced tumor cells with necrosis, degenerated eosinophilic tumor cells with fragmented nuclei (arrow) in the right half of the figure, and creeping fibrosis (arrows).

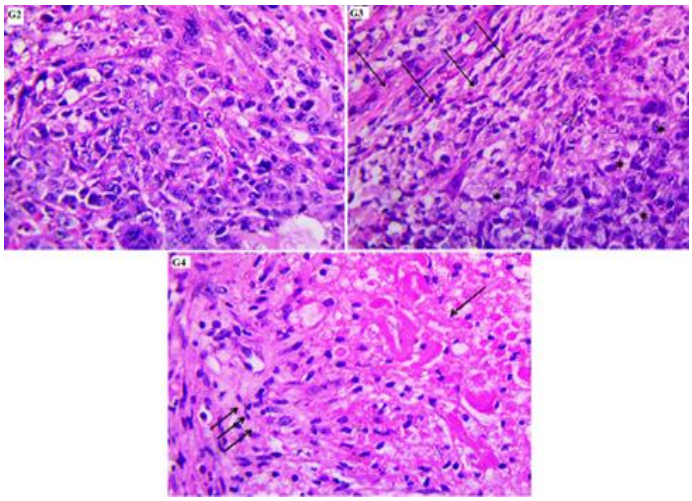

Fig. 6. Histopathological examination of tumor tissues of G2: section in control Ehrlich group showing viable undifferentiated tumor cells with marked pleomorphism, hyperchromatism, increased nuclear cytoplasmic ratio, prominent nucleoli and frequent mitosis (H&Ex400), G3: section in doxorubicin- treated group showing remaining viable tumor cells with prominent features of malignancy in the lower right corner (*) with fibroblasts and fibrosis encroaching on tumor cells (arrows) (H&Ex400), and G4: section in doxorubicin-loaded kaolinite- treated group showing replacement of tumor cells by necrosis, degenerated eosinophilic tumor cells with fragmented nuclei (arrow) in the right half of the figure together with creeping fibrosis (arrows) (H&Ex400

3.4. Safety of formulation

3.4.1. Kaolinite reduced the cancer-induced oxidative stress.

The levels of oxidative stress in the liver were assessed in all experimental groups. The levels of MDA were measured as an indicator of lipid peroxidation, and the levels of GSH and SOD were measured to evaluate antioxidant levels. According to Figure 7, the untreated G2 group had the highest levels of MDA compared to the other three groups. The group treated with doxorubicin

loaded kaolinite (G4) showed lower levels of MDA compared to the groups treated with saline (G2) or doxorubicin alone (G3), and slightly higher levels than the liver of naïve mice in G1. While G3 also displayed a significant drop in MDA levels, it was not as pronounced as in G4. Conversely, G2 had the lowest levels of antioxidants compared to G1, G3, and G4. The increase in antioxidant levels in G4 was remarkable and statistically significant compared to the positive control (G2)

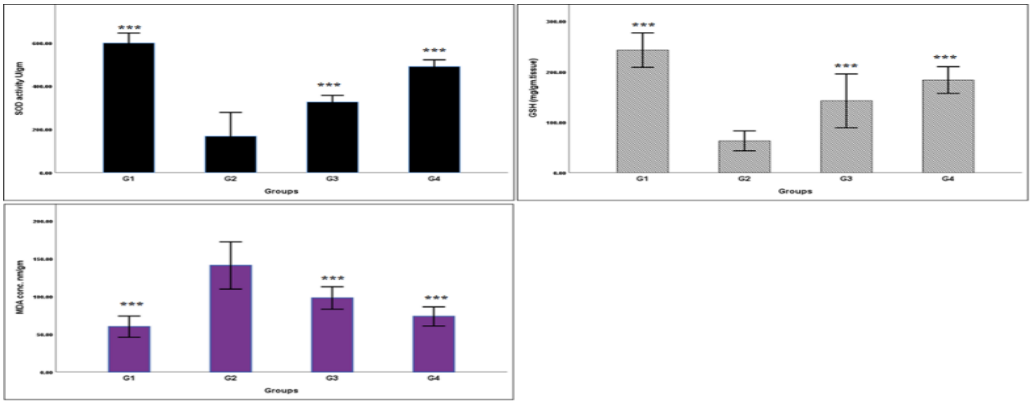

Fig. 7.SOD activity, GSH levels and MDA levels in the liver tissues of all the experimental groups.

3.4.2. Kaolinite prevented inflammation as well as cancer cell metastasis:

The histopathological examination of the livers of all the experimental groups was performed to confirm the oxidative stress data previously illustrated. As depicted in Fig. 8, G1 shows the standard histological structure of the liver parenchyma (H&E), whereas G2 shows random inflammatory cell infiltration with metastatic neoplastic cells (arrow). G3 also shows focal aggregation of inflammatory cells and necrobiotic alterations in the existing hepatocytes (H&E).G4 demonstrates seemingly normal liver tissue (H&E).

3.4.3. Kaolinite reduced genotoxicity in tumor-bearing mice

The comet assay results show that the G2 group had the highest proportion of liver DNA damage, followed by the G3 and G4 groups, as depicted in Fig.9. Hepatic cells in the G2 group had considerably longer comet tails than mice in the G1, G3, or G4 groups. Furthermore, the study discovered that the G3 group had a comet tail length significantly less than the G2 group but longer than the G4 and G1 groups. The tail and olive tail moments of the G1 and G4 groups were similar but lower than those of the G2 and G3 groups. The comet photos confirm the previous findings. The G2 group (Fig. 9(b)) displays irregular ghost-like formations, while the G3 group, exposed to doxorubicin, displays both intact and irregular shapes. This contrasts with the fully circular structures identified in the nuclei of the G1 and G4 livers (Fig. 9(a & d)).

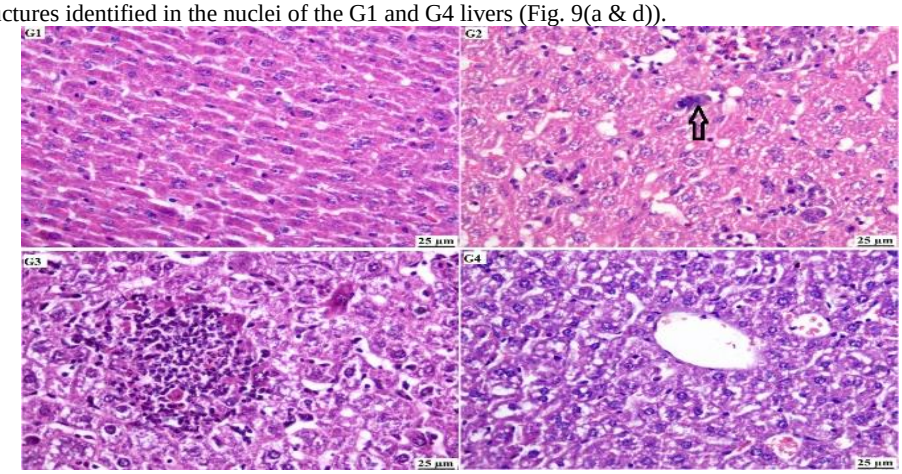

Fig.8. Photomicrograph of liver, G1 showing normal histological structure of hepatic parenchyma (H&E), G2 showing portal inflammatory cells infiltration with metastatic anaplastic tumor cells (H&E), G3: focal aggregation of inflammatory cells with necrobiotic changes of the existed hepatocytes (H&E), G3: showing apparently normal hepatic tissue (H&E).

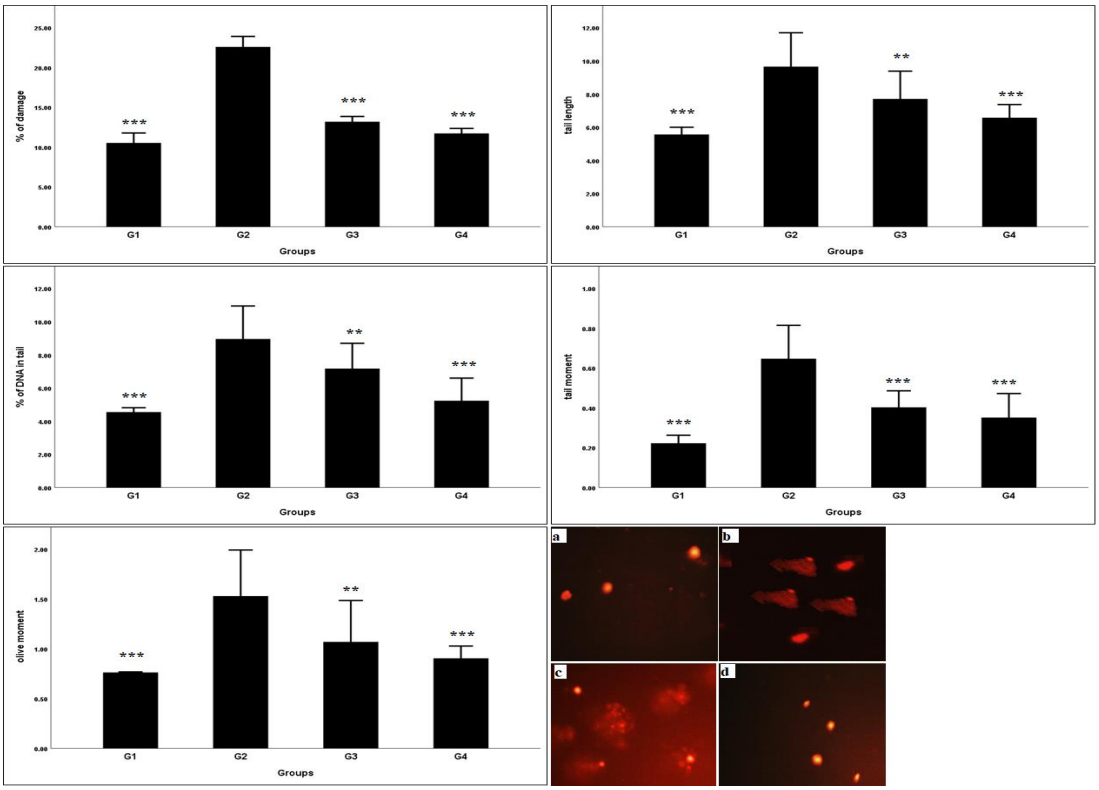

Fig.9. Comet parameters and comet images of livers of all the experimental group

3.4.4. Kaolinite prevented hemolysis of red blood cells (RBCs):

The hemolytic properties of doxorubicin-loaded kaolinite nanoparticles were studied at different doses (6.25, 12.5, 25, 50, and 100 µg/ml). Distilled water and saline solutions were used as positive and negative controls. The positive control tube showed the highest hemoglobin concentration in the supernatant, while the negative control showed zero hemolysis. According to Figure 10, the percentage of hemolysis ranged from 0.00% to 3.18%, below the threshold of 5%, after an hour of incubation with nanoparticles.

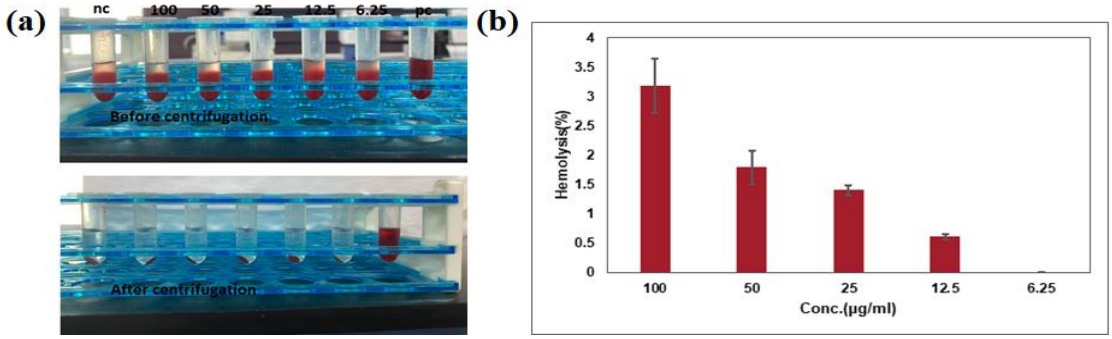

Fig.10. Hemolysis assay with doxorubicin-loaded kaolinite nanoparticles. a: The photograph depicts hemolys is in the human erythrocyte experiment following incubation with varying doses of doxorubicin-loaded kaolinite (6.25, 12.5, 50, and 100 µg/ml). Images of samples after 5 minutes of centrifugation at 10,000 rpm: negative control (nc, saline), positive control (pc, water). b: Hemolysis percentage at different concentrations of doxorubicin-loaded kaolinite. The data is shown as mean ±SD (n = 3).

4. Discussion

The importance of this study is highlighted by shedding light on the novelty of the examination of the anti-cancer effects of doxorubicin-loaded kaolinite against Ehrlich solid tumors as a breast cancer model. The study also examined their cytotoxic and genotoxic potentials against the liver as a vital organ. Moreover, the hemocompatibility of the formulation was assessed

to assure its safety for in vivo application. The formulation preparation process involved intercalating raw kaolinite with DMSO and methanol and loading it with doxorubicin. Intercalating kaolinite expands the interlayer area available for drug loading, as kaolinite is composed of multiple stacking layers of silicon SiO_4 tetrahedrons connected via strong hydrogen bonds to aluminum $AlO_2(OH)_4$octahedrons [37]. DMSO plays a vital role in the process by interacting with the hydroxyl groups of the exterior octahedron of kaolinite. The two methyl groups in the DMSO molecule form supplementary bonds with the oxygen atoms on the tetrahedral surface, allowing DMSO to organize itself between the kaolinite layers and providing sites for methanol. Afterward, DMSO is replaced with methanol, which provides negative charges to the kaolinite [38-40]. These intercalation processes increase the interlayer spaces available for subsequent drug loading [41]. The negatively charged methanol-intercalated kaolinite is then loaded with the cationic drug doxorubicin via electrostatic interaction, resulting in high loading efficiency [42]. This high loading efficiency indicates that the intercalation process was successful, allowing drug molecules to adsorb to the kaolinite nanoparticles' surfaces and in the spaces between the layers [43]. The nanoparticles were well-prepared and exhibited proper physico-chemical characteristics such as size, charge, and pH-dependent release. For example, the TEM and DLS data indicated that the particles were on an appropriate nanometer scale (less than 200nm), which enhanced their circulation time and cell absorption [17]. Reduction of the size of kaolinite to nanometer size occurs through the expansion of interlayer spaces via the intercalation process. As the interlayer gap of kaolinite expands upon intercalation, the level of structural disorder lessens, and the strength of interlayer bonding diminishes. This process leads to the fragmentation of kaolinite, producing smaller particles with a higher surface area and better dispersibility [44]. Furthermore, the reduction in size to the nanometer scale causes a decrease in crystallinity, as confirmed by the TEM images [45]. Additionally, the shift of the kaolinite nanoparticles' charge to positive after doxorubicin loading, indicates that the drug loading process worked appropriately, matching the high loading efficiency. Moreover, the in vivo experiment revealed a significant regression in tumor size, which was enhanced by the histopathological micrograph. The images showed remarkable necrosis in tumor tissues for G4, treated with the doxorubicin-loaded kaolinite nanoparticles, compared to G3, treated with free doxorubicin. The significant difference between the two groups is attributed to many possible modes of action. The main reason is the enhanced drug delivery to the tumor. For instance, the nanoparticles' proper physicochemical properties improved their drug delivery to the target. The positively charged nanoparticles have a high affinity for tumor cells' negatively charged cell membranes, allowing them to be easily transferred across them [46,47]. Additionally, the leaky vasculature of tumor cells enables the preferential accumulation of nanoparticles through the (EPR) effect [8]. Also, their size falls within the optimal range for internalization by tumor cells via the EPR effect [48]. Moreover, nanoparticles have a pH-dependent drug release mechanism that is effective within the acidic microenvironment of tumors. Another factor is the synergistic effect of kaolinite nanoparticles due to their surface silanol and aluminous groups that possess membranolytic activity, which breaks the membranes of tumor cells, leading to cell necrosis. This effect is augmented when combined with doxorubicin, which can intercalate the DNA base pairs within the cells, blocking both RNA and DNA replication and ultimately reducing tumor size [49,50]. Furthermore, kaolinite has been found to modulate the tumor microenvironment by reducing oxidative stress and inflammation, which prevent proliferation and metastasis of tumor [51]. In contrast, the decrease in the effectiveness of doxorubicin may be due to the non-specific accumulation of the medication in areas other than the intended target sites [52]. Another possibility is that cancer cells resist the treatment, a common disadvantage of using doxorubicin as a single therapy [53]. This resistance occurs because of a decrease in drug concentration within the nucleus of cancer cells, caused by efflux pumps that actively release the medication outside the cell. Consequently, the reduced drug concentration diminishes its ability to cause DNA damage, allowing cancer cells to continue their growth [53-55]. As high proportions of nanoparticles accumulate and are sequestered within the liver, the safety of nanoparticles was evaluated by examining their cyto/genotoxic effects on the liver of all the experimental groups [56]. One of the critical determinants of liver injury is oxidative stress [57]. Oxidative stress arises when the concentration of cellular antioxidants is surpassed by free radicals, including reactive oxygen species (ROS). This condition has detrimental effects on crucial cellular components, such as lipids, proteins, and nucleic acids, resulting in damage and various pathological conditions [58,59]. The notable increase in MDA levels and decrease in GSH and SOD observed in the G2 group can be attributed to the presence of the Ehrlich tumor model. This model is recognized for its ability to produce significant amounts of reactive oxygen species (ROS), which can cause tissue damage by reducing antioxidants and increasing lipid peroxidation products in essential organs [60]. Tumor cells generate elevated levels of reactive oxygen species (ROS) for various reasons, primarily due to heightened metabolic activity caused by mitochondrial dysfunction. This metabolic activity involves utilizing lactate as a substrate in the citric acid cycle when glucose is scarce, as observed in certain types of cancer, including breast cancer [61]. Furthermore, mutations in some enzymes in the tricarboxylic acid (TCA) cycle, such as succinate dehydrogenase and isocitrate dehydrogenase, increase the formation of reactive oxygen species (ROS) and tumor development [62]. Insufficient levels of antioxidants can accumulate excessive reactive oxygen species (ROS), which can cause lipid peroxidation. This process generates higher amounts of malondialdehyde (MDA). Moreover, oxidative stress amplifies cancer cell growth and spreads cancer cells to other body parts [63,64]. This induced oxidative stress matched the histopathological analysis of the untreated G2 group, which showed metastasis. The same finding of metastasis and portal inflammatory cell infiltration in untreated

mice was found in a study conducted by Jabir and his colleagues [65]. The absence of inflammation and necrosis in the group treated with doxorubicin-loaded nanoparticles, compared to those treated with doxorubicin alone, suggests that the nanoparticle formulation was more effective and safer. Doxorubicin can cause liver damage by disrupting hemostasis, lowering antioxidants, and increasing ROS levels. Additionally, with the depletion in GSH levels, ROS scavengers elevated the oxidative stress levels in the liver cells, promoting inflammation and DNA damage and leading to cell death [66]. The induced imbalance due to doxorubicin leads to the oxidation of lipids, DNA, and other biomolecules and tissue damage, resulting in inflammation and necrosis [67,68]. On the contrary, the encapsulation of doxorubicin in kaolinite-based nanoparticles significantly reduced the drug's side effects by releasing the drug into the targeted tumor. The oxidative stress and histopathological data highlight kaolinite's antioxidant and anti-inflammatory properties, align with the previously mentioned data in [14,69], and confirm that kaolinite's antioxidant and anti-inflammatory effects contribute to its anti-cancer properties. The antioxidant activity of kaolinite may be because the cations in kaolinite (K^{+}, Mg^{+2}, and Ca^{+2}) can neutralize oxide ions. Furthermore, the large specific surface area and high surface charge of kaolinite nanoclays help cancer cells adhere to the extracellular matrix, preventing their spread (metastasis) [70,71]. In addition, the high surface area, porous structure, and adsorption properties of kaolinite likely contribute to its antioxidant activities by reducing the concentration of free radicals and alleviating oxidative stress, which prevents tissue damage [16]. The antioxidant activity of kaolinite also helps reduce inflammation, as oxidative stress promotes the production of inflammation mediators [23]. In addition, the anti-inflammatory ability of kaolinite may be attributed to its capacity to adsorb and neutralize pro-inflammatory molecules and modulators due to its high surface area. Kaolinite has been previously reported to have topical anti-inflammatory and anti-analgesic effects [72]. It may be attributed to the ability of kaolinite to modulate immune cell activity by inhibiting the release of pro-inflammatory cytokines (IL-1β, TNF-α, and IL-6) and promoting the secretion of anti-inflammatory cytokines (IL-10). This balance between pro-inflammatory and anti-inflammatory cytokines contributes to the overall anti-inflammatory effect of kaolinite [73-75]. The data obtained from oxidative stress, histopathology, and comet assays consistently corroborate the findings in all groups. These findings enhance comprehension of the observed DNA damage in both G2 and G3, as confirmed by the degree of cell destruction and tail length [76]. The data for G2 and G3 demonstrated the highest levels of DNA damage, which may be attributed to the oxidative stress induced by the state of tumorigenesis, which causes damage to biomolecules like DNA [77]. High levels of MDA that are not enzymatically processed can damage DNA and various biomolecules by interacting covalently with proteins, forming DNA-protein crosslinks, and forming multiple adducts. Additionally, the interactions of MDA with biomolecules form epitopes, which stimulate various pro-inflammatory molecules, activating several downstream inflammation pathways [78-80]. Additionally, our findings of necrosis in the histopathology micrograph, mainly for G2 and G3, may be explained by the fact that the production of ROS, extended stimulation of Jun N-terminal kinase (JNK), and activation of poly(ADP-ribose) polymerase-1 (PARP-1) resulted in necrotic cell death [81]. In contrast, the normal histopathological photos of the liver of G4 that was treated with doxorubicin-loaded kaolinite emphasize the capacity of our formulation to mitigate the harmful effects of oxidative stress caused by solid tumors on the liver and accord with the observed reduction in DNA damage, inflammation, and absence of tissue death. Furthermore, we evaluated the hemolytic percentage of various concentrations of nanoparticles, a standard test for assessing the in vivo use of nanoparticles. RBCs destruction indicates toxicity as their destruction leads to the release of hemoglobin and causes hemoglobinuria through urination, which is a sign of blood poisoning. Additionally, nanoparticles can also cause hemagglutination by binding to red blood cells, which can have adverse effects such as hindering the normal functions of RBCs, blocking blood cells, and disrupting the osmolality of the blood. Due to these concerns, we studied the hemocompatibility of our formulation with human blood, particularly hemolysis. The data indicated that our nanoparticles were safe and hemocompatible, inducing a critical safe hemolytic ratio of less than 5% hemolysis [25,26]. The minimal hemolysis also suggests that the kaolinite nanoparticles did not cause oxidative stress in red blood cells, adding to their safety and antioxidant properties [82].

5. Conclusion

Our formulation offers triple benefits: anti-cancer, antioxidant, and anti-inflammatory properties. The nanoparticles are also confirmed to be safe for in vivo applications, with hemocompatibility. These advantages make it a promising candidate for more effective and safer cancer therapies, encouraging its use as an alternative to chemotherapy.

Funding sources
None

Declaration of competing interest
The authors declare that there is no conflict of interest.

References:

[1] Abdel Rahman AA, Sobhy A, Hawata MA, Zayed EM, Awad HM, El-Sayed WA. Synthesis and Anticancer Activity Evaluation of New 1, 2, 4-Triazolyl-Quinazoline Hybrid Compounds and Their Pyrazolopyridine Analogs. Egyptian Journal of Chemistry. 2024 Dec 1;67(13):393-402.

[2] El Tabl A, Abdel Wahed M, El Assaly MM, Ashour A. Nano-organometallic complexes as therapeutic platforms against breast cancer cell lines;(in vitro study). Egyptian Journal of Chemistry. 2021 Mar 1;64(3):1627-37.
[3] Galluzzi L, Humeau J, Buqué A, Zitvogel L, Kroemer G. Immunostimulation with chemotherapy in the era of immune checkpoint inhibitors. Nature reviews Clinical oncology. 2020 Dec;17(12):725-41.
[4] Joseph TM, Kar Mahapatra D, Esmaeili A, Piszczyk Ł, Hasanin MS, Kattali M, Haponiuk J, Thomas S. Nanoparticles: Taking a unique position in medicine. Nanomaterials. 2023 Jan 31;13(3):574.
[5] Shaaban A, Salem A, Elramly F, Ahmed E, Moawed F, Hegazy MG. Newly Created Hybrid Nanomaterial for Treatment of Lung Carcinoma. Egyptian Journal of Chemistry. 2022 Dec 1;65(131):1543-50.
[6] Tian H, Zhang T, Qin S, Huang Z, Zhou L, Shi J, Nice EC, Xie N, Huang C, Shen Z. Enhancing the therapeutic efficacy of nanoparticles for cancer treatment using versatile targeted strategies. Journal of hematology & oncology. 2022 Sep 12;15(1):132.
[7] Mastria EM, Cai LY, Kan MJ, Li X, Schaal JL, Fiering S, Gunn MD, Dewhirst MW, Nair SK, Chilkoti A. Nanoparticle formulation improves doxorubicin efficacy by enhancing host antitumor immunity. Journal of Controlled Release. 2018 Jan 10;269:364-73.
[8] Shukla T, Upmanyu N, Pandey SP, Sudheesh MS. Site-specific drug delivery, targeting, and gene therapy. InNanoarchitectonics in Biomedicine 2019 Jan 1 (pp. 473-505). William Andrew Publishing.
[9] Rozhina E, Batasheva S, Miftakhova R, Yan X, Vikulina A, Volodkin D, Fakhrullin R. Comparative cytotoxicity of kaolinite, halloysite, multiwalled carbon nanotubes and graphene oxide. Applied Clay Science. 2021 May 1;205:106041.
[10] Mitchell MJ, Billingsley MM, Haley RM, Wechsler ME, Peppas NA, Langer R. Engineering precision nanoparticles for drug delivery. Nature reviews drug discovery.
[11] Li K, Li D, Zhao L, Chang Y, Zhang Y, Cui Y, Zhang Z. Calcium-mineralized polypeptide nanoparticle for intracellular drug delivery in osteosarcoma chemotherapy. Bioactive Materials. 2020 Sep 1;5(3):721-31.
[12] Xie W, Chen Y, Yang H. Layered Clay Minerals in Cancer Therapy: Recent Progress and Prospects. Small. 2023 Aug;19(34):2300842.
[13] Awad ME, López-Galindo A, Setti M, El-Rahmany MM, Iborra CV. Kaolinite in pharmaceutics and biomedicine. International Journal of Pharmaceutics. 2017 Nov 25;533(1):34-48.
[14] Zhang Y, Long M, Huang P, Yang H, Chang S, Hu Y, Tang A, Mao L. Intercalated 2D nanoclay for emerging drug delivery in cancer therapy. Nano Research. 2017 Aug;10:2633-43.
[15] Gianni E, Avgoustakis K, Papoulis D. Kaolinite group minerals: Applications in cancer diagnosis and treatment. European Journal of Pharmaceutics and Biopharmaceutics. 2020 Sep 1;154:359-76
[16] Wu Q, Liao J, Yang H. Recent advances in kaolinite nanoclay as drug carrier for bioapplications: a review. Advanced Science. 2023 Sep;10(25):2300672.
[17] Khatoon N, Chu MQ, Zhou CH. Nanoclay-based drug delivery systems and their therapeutic potentials. Journal of Materials Chemistry B. 2020;8(33):7335-51.
[18] Zhang Y, Huang P, Long M, Liu S, Yang H, Yuan S, Chang S. Intercalated kaolinite as an emerging platform for cancer therapy. Science China Chemistry. 2019 Jan;62:58-61.
[19] Abukhadra MR, Allah AF. Synthesis and characterization of kaolinite nanotubes (KNTs) as a novel carrier for 5-fluorouracil of high encapsulation properties and controlled release. Inorganic Chemistry Communications. 2019 May 1;103:30-6.
[20] Wei G, He W, Bai Y, Yu H. WITHDRAWN: Design and evaluation of a novel Kaolin-chitosan/gold nanocomposite for the treatment of human lung cancer.
[21] Dong W, Zhang J, Zhuang Z, Zhong J, Zhang J. Formulation of a novel anti-human oral squamous cell carcinoma supplement by gold nanoparticles-Kaolin nanocomposite. Journal of Experimental Nanoscience. 2022 Dec 31;17(1):138-49.
[22] Zhang D, Wang L, Tian L, Chen W, El-kott AF, Negm S, Eltantawy W, Alshaharni MO. Bio-inspired deposition of gold nanoparticles onto the surface of kaolin for in vitro management of human ovarian cancer and modulation of the inflammatory response in adenomyosis-induced mice in vivo via the MAPK signaling pathway. Journal of Science: Advanced Materials and Devices. 2024 Jun 1;9(2):100714
[23] Hussain T, Tan B, Yin Y, Blachier F, Tossou MC, Rahu N. Oxidative stress and inflammation: what polyphenols can do for us?. Oxidative medicine and cellular longevity. 2016 Oct;2016.
[24] El Yamani N, Rundén-Pran E, Collins AR, Longhin EM, Elje E, Hoet P, Vinković Vrček I, Doak SH, Fessard V, Dusinska M. The miniaturized enzyme-modified comet assay for genotoxicity testing of nanomaterials. Frontiers in Toxicology. 2022 Oct 12;4:986318.
[25] Mazzarino L, Loch-Neckel G, dos Santos Bubniak L, Ourique F, Otsuka I, Halila S, Curi Pedrosa R, Santos-Silva MC, Lemos-Senna E, Curti Muniz E, Borsali R. Nanoparticles made from xyloglucan-block-polycaprolactone copolymers: Safety assessment for drug delivery. Toxicological Sciences. 2015 Sep 1;147(1):104-15.
[26] Yin G, Zhao D, Wang X, Ren Y, Zhang L, Wu X, Nie S, Li Q. Bio-compatible poly (ester-urethane) s based on PEG–PCL–PLLA copolymer with tunable crystallization and bio-degradation properties. RSC advances. 2015;5(96):79070-80.
[27] Monem AS, Elbialy N, Mohamed N. Mesoporous silica coated gold nanorods loaded doxorubicin for combined chemo–photothermal therapy. International journal of pharmaceutics. 2014 Aug 15;470(1-2):1-7.
[28] Li HF, Wu C, Xia M, Zhao H, Zhao MX, Hou J, Li R, Wei L, Zhang L. Targeted and controlled drug delivery using a temperature and ultra-violet responsive liposome with excellent breast cancer suppressing ability. RSC advances. 2015;5(35):27630-9.
[29] Akhila JS, Shyamjith D, Alwar MC. Acute toxicity studies and determination of median lethal dose. Current science. 2007 Oct 10:917-20.
[30] Chinedu E, Arome D, Ameh FS. A new method for determining acute toxicity in animal models. Toxicology international. 2013 Sep;20(3):224.

[31]Tolba MF, Sedky NK, Ali MA, Abdollah MR. Modeling neurotoxin-induced neuroinflammation with chemotherapy. InHandbook of Animal Models in Neurological Disorders 2023 Jan 1 (pp. 403-417). Academic Press
[32]Elbialy NS, Mady MM. Ehrlich tumor inhibition using doxorubicin containing liposomes. Saudi Pharmaceutical Journal. 2015 Apr 1;23(2):182-7.
[33]Ohkawa H, Ohishi N, Yagi K. Assay for lipid peroxides in animal tissues by thiobarbituric acid reaction. Analytical biochemistry. 1979 Jun 1;95(2):351-8.
[34]Beutler E, Kelly BM. The effect of sodium nitrite on red cell GSH. Experientia. 1963 Feb;19(2):96-7.
[35]Nishikimi M, Rao NA, Yagi K. The occurrence of superoxide anion in the reaction of reduced phenazine methosulfate and molecular oxygen. Biochemical and biophysical research communications. 1972 Jan 31;46(2):849-54.
[36]Zhang J, Chen XG, Li YY, Liu CS. Self-assembled nanoparticles based on hydrophobically modified chitosan as carriers for doxorubicin. Nanomedicine: Nanotechnology, Biology and Medicine. 2007 Dec 1;3(4):258-65.
[37]Zuo X, Wang D, Zhang S, Liu Q, Yang H. Intercalation and exfoliation of kaolinite with sodium dodecyl sulfate. Minerals. 2018 Mar 9;8(3):112.
[38]Zhang S, Liu Q, Cheng H, Gao F, Liu C, Teppen BJ. Mechanism responsible for intercalation of dimethyl sulfoxide in kaolinite: Molecular dynamics simulations. Applied clay science. 2018 Jan 1;151:46-53.
[39]Qu H, He S, Su H. Efficient preparation of kaolinite/methanol intercalation composite by using a Soxhlet extractor. Scientific reports. 2019 Jun 6;9(1):8351.
[40]Michalkova A, Tunega D. Kaolinite: dimethylsulfoxide intercalate A theoretical study. The Journal of Physical Chemistry C. 2007 Aug 2;111(30):11259-66.
[41]Tan D, Yuan P, Dong F, He H, Sun S, Liu Z. Selective loading of 5-fluorouracil in the interlayer space of methoxy-modified kaolinite for controlled release. Applied Clay Science. 2018 Jun 1;159:102-6.
[42]Zhang S, Liu Q, Cheng H, Zhang Y, Li X, Frost RL. Intercalation of γ-aminopropyl triethoxysilane (APTES) into kaolinite interlayer with methanol-grafted kaolinite as intermediate. Applied Clay Science. 2015 Sep 1;114:484-90.
[43]Liao J, Qian Y, Sun Z, Wang J, Zhang Q, Zheng Q, Wei S, Liu N, Yang H. In Vitro Binding and Release Mechanisms of Doxorubicin from Nanoclays. The Journal of Physical Chemistry Letters. 2022 Sep 2;13(36):8429-35.
[44]Lagaly G, Ogawa M, Dékány I. Clay mineral–organic interactions. InDevelopments in clay science 2013 Jan 1 (Vol. 5, pp. 435-505). Elsevier.
[45]Ndzana GM, Huang L, Zhang Z, Zhu J, Liu F, Bhattacharyya R. The transformation of clay minerals in the particle size fractions of two soils from different latitude in China. Catena. 2019 Apr 1;175:317-28.
[46]Yang R, Shim WS, Cui FD, Cheng G, Han X, Jin QR, Kim DD, Chung SJ, Shim CK. Enhanced electrostatic interaction between chitosan-modified PLGA nanoparticle and tumor. International journal of pharmaceutics. 2009 Apr 17;371(1-2):142-7.
[47]Forest V, Pourchez J. Preferential binding of positive nanoparticles on cell membranes is due to electrostatic interactions: A too simplistic explanation that does not take into account the nanoparticle protein corona. Materials Science and Engineering: C. 2017 Jan 1;70:889-96.
[48]Fan D, Cao Y, Cao M, Wang Y, Cao Y, Gong T. Nanomedicine in cancer therapy. Signal Transduction and Targeted Therapy. 2023 Aug 7;8(1):293.
[49]Cananà S, Pavan C, Bellomo C, Escolano-Casado G, Chilla G, Lison D, Mino L, Turci F. Interaction of Layered Silicates with Biomembranes: Ion Exchangers and Non-Exchangers. Advanced Materials Interfaces. 2022 Oct;9(29):2201347.
[50]Johnson-Arbor K, Dubey R. Doxorubicin.
[51]Arfin S, Jha NK, Jha SK, Kesari KK, Ruokolainen J, Roychoudhury S, Rathi B, Kumar D. Oxidative stress in cancer cell metabolism. Antioxidants. 2021 Apr 22;10(5):642.
[52]Dragojevic S, Ryu JS, Hall ME, Raucher D. Targeted drug delivery biopolymers effectively inhibit breast tumor growth and prevent doxorubicin-induced cardiotoxicity. Molecules. 2022 May 24;27(11):3371.
[53]Cao WQ, Li Y, Hou YJ, Yang MX, Fu XQ, Zhao BS, Jiang HM, Fu XY. Enhanced anticancer efficiency of doxorubicin against human glioma by natural borneol through triggering ROS-mediated signal. Biomedicine & Pharmacotherapy. 2019 Oct 1;118:109261.
[54]Elbialy NS, Mady MM. Ehrlich tumor inhibition using doxorubicin containing liposomes. Saudi Pharmaceutical Journal. 2015 Apr 1;23(2):182-7.
[55]Cox J, Weinman S. Mechanisms of doxorubicin resistance in hepatocellular carcinoma. Hepatic oncology. 2016 Jan;3(1):57-9.
[56]Zhang YN, Poon W, Tavares AJ, McGilvray ID, Chan WC. Nanoparticle–liver interactions: Cellular uptake and hepatobiliary elimination. Journal of controlled release. 2016 Oct 28;240:332-48.
[57]Arauz J, Ramos-Tovar E, Muriel P. Redox state and methods to evaluate oxidative stress in liver damage: From bench to bedside. Annals of Hepatology. 2016 Feb 15;15(2):160-73.
[58]Sajnani K, Islam F, Smith RA, Gopalan V, Lam AK. Genetic alterations in Krebs cycle and its impact on cancer pathogenesis. Biochimie. 2017 Apr 1;135:164-72.
[59]Pizzino G, Irrera N, Cucinotta M, Pallio G, Mannino F, Arcoraci V, Squadrito F, Altavilla D, Bitto A. Oxidative stress: harms and benefits for human health. Oxidative medicine and cellular longevity. 2017 Oct;2017.
[60]Sadiq IZ. Free radicals and oxidative stress: signaling mechanisms, redox basis for human diseases, and cell cycle regulation. Current molecular medicine. 2023 Jan 1;23(1):13-35.
[61]Aldubayan MA, Elgharabawy RM, Ahmed AS, Tousson E. Antineoplastic activity and curative role of avenanthramides against the growth of ehrlich solid tumors in mice. Oxidative medicine and cellular longevity. 2019 Jan 13;2019.
[62]Schiliro C, Firestein BL. Mechanisms of metabolic reprogramming in cancer cells supporting enhanced growth and proliferation. Cells. 2021 Apr 29;10(5):1056.
[63]Barrera G. Oxidative stress and lipid peroxidation products in cancer progression and therapy. International Scholarly Research Notices. 2012;2012.

[64]Ellethy AT. Potential antitumor activity of nonsteroidal anti-inflammatory drugs against Ehrlich ascites carcinoma in experimental animals. International journal of health sciences. 2019 Sep;13(5):11.
[65]Jabir MS, Abood NA, Jawad MH, Öztürk K, Kadhim H, Albukhaty S, Al-Shammari A, AlMalki FA, Albaqami J, Sulaiman GM. Gold nanoparticles loaded TNF-α and CALNN peptide as a drug delivery system and promising therapeutic agent for breast cancer cells. Materials Technology. 2022 Dec 6;37(14):3152-66.
[66]Jabir MS, Mohammed MK, Albukhaty S, Ahmed DS, Syed A, Elgorban AM, Eswaramoorthy R, Al-kuraishy HM, Al-Gareeb AI, Ghotekar S, Jawad SF. Functionalized SWCNTs@ Ag–TiO2 nanocomposites induce ROS-mediated apoptosis and autophagy in liver cancer cells. Nanotechnology Reviews. 2023 Oct 28;12(1):20230127.
[67]Song S, Chu L, Liang H, Chen J, Liang J, Huang Z, Zhang B, Chen X. Protective effects of dioscin against doxorubicin-induced hepatotoxicity via regulation of Sirt1/FOXO1/NF-κb signal. Frontiers in pharmacology. 2019 Sep 13;10:1030.
[68]AlAsmari AF, Alharbi M, Alqahtani F, Alasmari F, AlSwayyed M, Alzarea SI, Al-Alallah IA, Alghamdi A, Hakami HM, Alyousef MK, Sari Y. Diosmin alleviates doxorubicin-induced liver injury via modulation of oxidative stress-mediated hepatic inflammation and apoptosis via NfkB and MAPK pathway: A preclinical study. Antioxidants. 2021 Dec 15;10(12):1998.
[69]LÓPEZ-GALINDO AL, Viseras C. Pharmaceutical and cosmetic applications of clays. InInterface science and technology 2004 Jan 1 (Vol. 1, pp. 267-289). Elsevier.
[70]Misyak SA, Burlaka AP, Golotiuk VV, Lukin SM, Kornienko PL. Antiradical, antimetastatic and antitumor activity of kaolin preparation "kremnevit". Galician Medical Journal. 2016 Mar 30;23(1):44-7.
[71]Abduljauwad SN, Ahmed HU, Moy VT. Melanoma treatment via non-specific adhesion of cancer cells using charged nano-clays in pre-clinical studies. Scientific reports. 2021 Feb 2;11(1):2737.
[72]Messina JM, Luo M, Hossan MS, Gadelrab HA, Yang X, John A, Wilmore JR, Luo J. Unveiling Cytokine Charge Disparity as a Potential Mechanism for Immune Regulation. Cytokine & Growth Factor Reviews. 2023 Dec 26.
[73]Copray JC, Mantingh I, Brouwer N, Biber K, Küst BM, Liem RS, Huitinga I, Tilders FJ, Van Dam AM, Boddeke HW. Expression of interleukin-1 beta in rat dorsal root ganglia. Journal of neuroimmunology. 2001 Aug 30;118(2):203-11.
[74]Wieseler-Frank J, Maier SF, Watkins LR. Glial activation and pathological pain. Neurochemistry international. 2004 Jul 1;45(2-3):389-95.
[75]Zhang JM, An J. Cytokines, inflammation, and pain. International anesthesiology clinics. 2007 Apr 1;45(2):27-37.
[76]Kadhim AA, Abbas NR, Kadhum HH, Albukhaty S, Jabir MS, Naji AM, Hamzah SS, Mohammed MK, Al-Karagoly H. Investigating the effects of biogenic zinc oxide nanoparticles produced using papaver somniferum extract on oxidative stress, cytotoxicity, and the induction of apoptosis in the THP-1 cell line. Biological Trace Element Research. 2023 Oct;201(10):4697-709.
[77]Czarny P, Wigner P, Galecki P, Sliwinski T. The interplay between inflammation, oxidative stress, DNA damage, DNA repair and mitochondrial dysfunction in depression. Progress in Neuro-Psychopharmacology and Biological Psychiatry. 2018 Jan 3;80:309-21.
[78]Marnett LJ. Lipid peroxidation—DNA damage by malondialdehyde. Mutation Research/Fundamental and Molecular Mechanisms of Mutagenesis. 1999 Mar 8;424(1-2):83-95.
[79]Voitkun V, Zhitkovich A. Analysis of DNA–protein crosslinking activity of malondialdehyde in vitro. Mutation Research/Fundamental and Molecular Mechanisms of Mutagenesis. 1999 Mar 8;424(1-2):97-106.
[80]Busch CJ, Binder CJ. Malondialdehyde epitopes as mediators of sterile inflammation. Biochimica et Biophysica Acta (BBA)-Molecular and Cell Biology of Lipids. 2017 Apr 1;1862(4):398-406.
[81]Borges HL, Linden R, Wang JY. DNA damage-induced cell death: lessons from the central nervous system. Cell research. 2008 Jan;18(1):17-26.
[82]Schaer DJ, Buehler PW, Alayash AI, Belcher JD, Vercellotti GM. Hemolysis and free hemoglobin revisited: exploring hemoglobin and hemin scavengers as a novel class of therapeutic proteins. Blood, The Journal of the American Society of Hematology. 2013 Feb21;121(8):1276-84.
[83]Molecular Mechanisms of Mutagenesis. 1999 Mar 8;424(1-2):97-106.
[84]Busch CJ, Binder CJ. Malondialdehyde epitopes as mediators of sterile inflammation. Biochimica et Biophysica Acta (BBA)-Molecular and Cell Biology of Lipids. 2017 Apr 1;1862(4):398-406.
[85]Borges HL, Linden R, Wang JY. DNA damage-induced cell death: lessons from the central nervous system. Cell research. 2008 Jan;18(1):17-26.
[86]Schaer DJ, Buehler PW, Alayash AI, Belcher JD, Vercellotti GM. Hemolysis and free hemoglobin revisited: exploring hemoglobin and hemin scavengers as a novel class of therapeutic proteins. Blood, The Journal of the American Society of Hematology. 2013 Feb 21;121(8):1276-84.